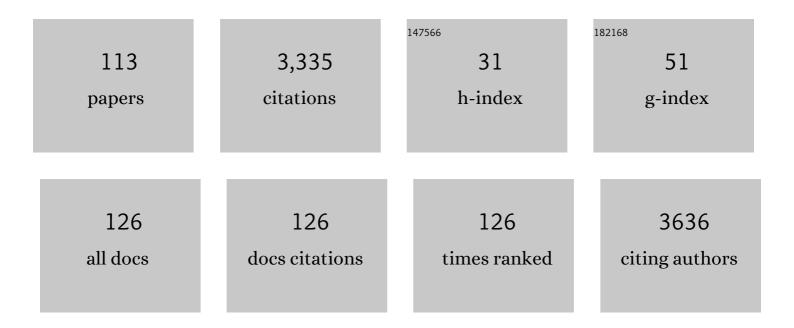
Wooyong Um

List of Publications by Year in descending order

Source: https://exaly.com/author-pdf/4227781/publications.pdf Version: 2024-02-01



WOOYONG LIM

#	Article	IF	CITATIONS
1	Partitioning effects and corrosion characteristics of oxyapatite glass-ceramic wasteforms sequestering rare-earth elements. Nuclear Engineering and Technology, 2022, 54, 997-1002.	1.1	1
2	Co2+/PMS based sulfate-radical treatment for effective mineralization of spent ion exchange resin. Chemosphere, 2022, 287, 132351.	4.2	22
3	Removal of iodine (Iâ^' and IO3â^') from aqueous solutions using CoAl and NiAl layered double hydroxides. Chemical Engineering Journal, 2022, 430, 132788.	6.6	9
4	Decontamination of radioactive metal wastes using underwater microwave plasma. Journal of Environmental Chemical Engineering, 2022, 10, 107090.	3.3	2
5	Metallic technetium sequestration in nickel core/shell microstructure during Fe(OH)2 transformation with Ni doping. Journal of Hazardous Materials, 2022, 425, 127779.	6.5	3
6	Comparative study of PMS oxidation with Fenton oxidation as an advanced oxidation process for Co-EDTA decomplexation. Chemosphere, 2022, 300, 134494.	4.2	16
7	The evolution of hydrated lime-based cementitious waste forms during leach testing leading to enhanced technetium retention. Journal of Hazardous Materials, 2022, 430, 128507.	6.5	4
8	Simultaneous removal of cesium and iodate using prussian blue functionalized CoCr layered double hydroxide (PB-LDH). Journal of Environmental Chemical Engineering, 2022, 10, 107477.	3.3	12
9	Kinetics and mechanism of rhenium-ethylenediaminetetraacetic acid (Re(IV)-EDTA) complex degradation; For 99Tc-EDTA degradation in the natural environment. Environmental Technology and Innovation, 2022, 27, 102492.	3.0	0
10	Fenton-like treatment for reduction of simulated carbon-14 spent resin. Journal of Environmental Chemical Engineering, 2021, 9, 104740.	3.3	7
11	Energy, safety, and absorption efficiency evaluation of a pilot-scale H2S abatement process using MDEA solution in a coke-oven gas. Journal of Environmental Chemical Engineering, 2021, 9, 105037.	3.3	6
12	Evaluating thermal stability of rare-earth containing wasteforms at extraordinary nuclear disposal conditions. Nuclear Engineering and Technology, 2021, 53, 2576-2581.	1.1	2
13	A Focused Ion Beam-Scanning Transmission Electron Microscopy with Energy-Dispersive X-ray Spectroscopy Study on Technetium Incorporation within Iron Oxides through Fe(OH) ₂ (s) Mineral Transformation. ACS Earth and Space Chemistry, 2021, 5, 525-534.	1.2	5
14	Development of a Geochemical Speciation Model for Use in Evaluating Leaching from a Cementitious Radioactive Waste Form. Environmental Science & Technology, 2021, 55, 8642-8653.	4.6	18
15	Inorganic Waste Forms for Efficient Immobilization of Radionuclides. ACS ES&T Engineering, 2021, 1, 1149-1170.	3.7	34
16	Process optimization and safety assessment on a pilot-scale Bunsen process in sulfur–iodine cycle. International Journal of Hydrogen Energy, 2021, 46, 33616-33634.	3.8	8
17	Development of geopolymer waste form for immobilization of radioactive borate waste. Journal of Hazardous Materials, 2021, 419, 126402.	6.5	30
18	Effect of ion exchange resin particle size on homogeneity and leachability of Cs and Co in polymer waste form. RSC Advances, 2021, 11, 2729-2732.	1.7	1

#	Article	IF	CITATIONS
19	Fenton and Fenton-like wet oxidation for degradation and destruction of organic radioactive wastes. Npj Materials Degradation, 2021, 5, .	2.6	24
20	Nanostructured MgFe and CoCr layered double hydroxides for removal and sequestration of iodine anions. Chemical Engineering Journal, 2020, 380, 122408.	6.6	47
21	Impact of Cr and Co on 99Tc retention in magnetite: A combined study of ab initio molecular dynamics and experiments. Journal of Hazardous Materials, 2020, 387, 121721.	6.5	3
22	Transport of Colloidal Particles in Microscopic Porous Medium Analogues with Surface Charge Heterogeneity: Experiments and the Fundamental Role of Single-Bead Deposition. Environmental Science & Technology, 2020, 54, 13651-13660.	4.6	7
23	Waterâ€dispersible nanocolloids and higher temperatures promote the release of carbon from riparian soil. Vadose Zone Journal, 2020, 19, e20077.	1.3	2
24	Charge transfer rhenium complexes analogue to pertechnetate removal. Journal of Environmental Chemical Engineering, 2020, 8, 104366.	3.3	1
25	Dissolved Carbonate and pH Control the Dissolution of Uranyl Phosphate Minerals in Flow-Through Porous Media. Environmental Science & Technology, 2020, 54, 6031-6042.	4.6	11
26	Relationship between leaching behavior and glass structure of calcium-aluminoborate waste glasses with various La2O3 contents. Journal of Nuclear Materials, 2020, 539, 152331.	1.3	3
27	Kinetics of Co-Mingled ⁹⁹ Tc and Cr Removal during Mineral Transformation of Ferrous Hydroxide. ACS Earth and Space Chemistry, 2020, 4, 218-228.	1.2	5
28	Investigation of 3H, 99Tc, and 90Sr transport in fractured rock and the effects of fracture-filling/coating material at LILW disposal facility. Environmental Geochemistry and Health, 2019, 41, 411-425.	1.8	4
29	Development of bismuth-functionalized graphene oxide to remove radioactive iodine. Dalton Transactions, 2019, 48, 478-485.	1.6	57
30	Relative permeability for water and gas through fractures in cement. PLoS ONE, 2019, 14, e0210741.	1.1	7
31	Temporal changes of geochemistry and microbial community in low and intermediate level waste (LILW) repository, South Korea. Annals of Nuclear Energy, 2019, 128, 309-317.	0.9	7
32	Development of metakaolin-based geopolymer for solidification of sulfate-rich HyBRID sludge waste. Journal of Nuclear Materials, 2019, 518, 247-255.	1.3	22
33	Insights into the physical and chemical properties of a cement-polymer composite developed for geothermal wellbore applications. Cement and Concrete Composites, 2019, 97, 279-287.	4.6	22
34	99Tc immobilization from off-gas waste streams using nickel-doped iron spinel. Journal of Hazardous Materials, 2019, 364, 69-77.	6.5	11
35	Synthesis of rhenium-doped tin dioxide for technetium radioactive waste immobilization. Journal of Nuclear Materials, 2018, 505, 134-142.	1.3	12
36	Effect of chemical and physical heterogeneities on colloid-facilitated cesium transport. Journal of Contaminant Hydrology, 2018, 213, 22-27.	1.6	14

#	Article	IF	CITATIONS
37	Magnetite-based adsorbents for sequestration of radionuclides: a review. RSC Advances, 2018, 8, 2521-2540.	1.7	57
38	Uranium speciation in acid waste-weathered sediments: The role of aging and phosphate amendments. Applied Geochemistry, 2018, 89, 109-120.	1.4	17
39	Dissolution of studtite [UO2(O2)(H2O)4] in various geochemical conditions. Journal of Environmental Radioactivity, 2018, 189, 57-66.	0.9	10
40	Effect of Technetium-99 sources on its retention in low activity waste glass. Journal of Nuclear Materials, 2018, 503, 235-244.	1.3	15
41	Effect of seawater intrusion on radioactive strontium (⁹⁰ Sr) sorption and transport at nuclear power plants. Radiochimica Acta, 2018, 106, 147-160.	0.5	6
42	Removal of Chalk River unidentified deposit (CRUD) radioactive waste by enhanced electrokinetic process. Journal of Industrial and Engineering Chemistry, 2018, 57, 89-96.	2.9	6
43	Cr(VI) Effect on Tc-99 Removal from Hanford Low-Activity Waste Simulant by Ferrous Hydroxide. Environmental Science & Technology, 2018, 52, 11752-11759.	4.6	11
44	Characterizing Technetium in Subsurface Sediments for Contaminant Remediation. ACS Earth and Space Chemistry, 2018, 2, 1145-1160.	1.2	8
45	Geochemical alteration of wellbore cement by CO ₂ or CO ₂ + H ₂ reaction during longâ€ŧerm carbon storage. , 2017, 7, 852-865.	S	17
46	Structure analysis of vitusite glass–ceramic waste forms using extended X-ray absorption fine structures. Ceramics International, 2017, 43, 4687-4691.	2.3	5
47	Synthesis of Tributyl Phosphate-Coated Hydroxyapatite for Selective Uranium Removal. Industrial & Engineering Chemistry Research, 2017, 56, 3399-3406.	1.8	21
48	Polymer-Cement Composites with Self-Healing Ability for Geothermal and Fossil Energy Applications. Chemistry of Materials, 2017, 29, 4708-4718.	3.2	28
49	Tellurite glasses for vitrification of technetium-99 from pyrochemical processing. Journal of Nuclear Materials, 2017, 493, 1-5.	1.3	15
50	Rates and mechanisms of uranyl oxyhydroxide mineral dissolution. Geochimica Et Cosmochimica Acta, 2017, 207, 298-321.	1.6	12
51	Uranium Release from Acidic Weathered Hanford Sediments: Single-Pass Flow-Through and Column Experiments. Environmental Science & Technology, 2017, 51, 11011-11019.	4.6	15
52	Enhanced 99Tc retention in glass waste form using Tc(IV)-incorporated Fe minerals. Journal of Nuclear Materials, 2017, 495, 455-462.	1.3	21
53	Superparamagnetic Adsorbent Based on Phosphonate Grafted Mesoporous Carbon for Uranium Removal. Industrial & Engineering Chemistry Research, 2017, 56, 9821-9830.	1.8	45
54	Reduction and Simultaneous Removal of ⁹⁹ Tc and Cr by Fe(OH) ₂ (s) Mineral Transformation. Environmental Science & Technology, 2017, 51, 8635-8642.	4.6	68

#	Article	IF	CITATIONS
55	Effects of hydrated lime on radionuclides stabilization of Hanford tank residual waste. Chemosphere, 2017, 185, 171-177.	4.2	3
56	Recyclable superparamagnetic adsorbent based on mesoporous carbon for sequestration of radioactive Cesium. Chemical Engineering Journal, 2017, 308, 798-808.	6.6	37
57	Impeding 99Tc(IV) mobility in novel waste forms. Nature Communications, 2016, 7, 12067.	5.8	94
58	Superparamagnetic nalidixic acid grafted magnetite (Fe ₃ O ₄ /NA) for rapid and efficient mercury removal from water. RSC Advances, 2016, 6, 35825-35832.	1.7	17
59	Computational Investigation of Technetium(IV) Incorporation into Inverse Spinels: Magnetite (Fe ₃ O ₄) and Trevorite (NiFe ₂ O ₄). Environmental Science & Technology, 2016, 50, 5216-5224.	4.6	32
60	Bead-Based Microfluidic Sediment Analogues: Fabrication and Colloid Transport. Langmuir, 2016, 32, 9342-9350.	1.6	5
61	Numerical Simulation of Permeability Change in Wellbore Cement Fractures after Geomechanical Stress and Geochemical Reactions Using X-ray Computed Tomography Imaging. Environmental Science & Technology, 2016, 50, 6180-6188.	4.6	14
62	Review: Role of chemistry, mechanics, and transport on well integrity in CO2 storage environments. International Journal of Greenhouse Gas Control, 2016, 49, 149-160.	2.3	141
63	Liquid Scintillation Counting Methodology for ⁹⁹ Tc Analysis: A Remedy for Radiopharmaceutical Waste. Analytical Chemistry, 2015, 87, 9054-9060.	3.2	7
64	Technetium Incorporation into Goethite (α-FeOOH): An Atomic-Scale Investigation. Environmental Science & Technology, 2015, 49, 13699-13707.	4.6	58
65	Sludge Reduction by H ₂ O ₂ Oxidation with Fe/MgO Catalyst. Water Environment Research, 2015, 87, 675-682.	1.3	1
66	Bench-scale electrokinetic remediation for cesium-contaminated sediment at the Hanford Site, USA. Journal of Radioanalytical and Nuclear Chemistry, 2015, 304, 615-625.	0.7	13
67	Reductive capacity measurement of waste forms for secondary radioactive wastes. Journal of Nuclear Materials, 2015, 467, 251-259.	1.3	12
68	Environmentally friendly, rheoreversible, hydraulic-fracturing fluids for enhanced geothermal systems. Geothermics, 2015, 58, 22-31.	1.5	26
69	Fracture Flow of Radionuclides in Unsaturated Conditions at LILW Disposal Facility. Daehan Hwan'gyeong Gonghag Hoeji, 2015, 37, 465-471.	0.4	0
70	Geochemical and Geomechanical Effects on Wellbore Cement Fractures. Energy Procedia, 2014, 63, 5808-5812.	1.8	8
71	Biogeochemical changes at early stage after the closure of radioactive waste geological repository in South Korea. Annals of Nuclear Energy, 2014, 71, 6-10.	0.9	9
72	Effects of Radiation and Temperature on Iodide Sorption by Surfactant-Modified Bentonite. Environmental Science & Technology, 2014, 48, 9684-9691.	4.6	57

#	Article	IF	CITATIONS
73	Influence of Phosphate and Silica on U(VI) Precipitation from Acidic and Neutralized Wastewaters. Environmental Science & Technology, 2014, 48, 6097-6106.	4.6	59
74	Effects of iron oxides on the rheological properties of cementitious slurry. Colloids and Surfaces A: Physicochemical and Engineering Aspects, 2014, 453, 94-100.	2.3	9
75	Chemical stabilization of Hanford tank residual waste. Journal of Nuclear Materials, 2014, 446, 246-256.	1.3	14
76	Development of iron phosphate ceramic waste form to immobilize radioactive waste solution. Journal of Nuclear Materials, 2014, 452, 16-23.	1.3	20
77	Wellbore cement fracture evolution at the cement–basalt caprock interface during geologic carbon sequestration. Applied Geochemistry, 2014, 47, 1-16.	1.4	50
78	Effect of oxygen co-injected with carbon dioxide on Gothic shale caprock–CO2–brine interaction during geologic carbon sequestration. Chemical Geology, 2013, 354, 1-14.	1.4	45
79	2D and 3D imaging resolution trade-offs in quantifying pore throats for prediction of permeability. Advances in Water Resources, 2013, 62, 1-12.	1.7	70
80	Facilitated strontium transport by remobilization of strontium-containing secondary precipitates in Hanfod Site subsurface. Journal of Hazardous Materials, 2013, 248-249, 364-370.	6.5	8
81	Imaging Wellbore Cement Degradation by Carbon Dioxide under Geologic Sequestration Conditions Using X-ray Computed Microtomography. Environmental Science & Technology, 2013, 47, 283-289.	4.6	48
82	The Effects of Secondary Mineral Precipitates on 90Sr Mobility at the Hanford Site, USA. Procedia Earth and Planetary Science, 2013, 7, 855-858.	0.6	1
83	Experimental study of potential wellbore cement carbonation by various phases of carbon dioxide during geologic carbon sequestration. Applied Geochemistry, 2013, 35, 161-172.	1.4	51
84	Setting and stiffening of cementitious components in Cast Stone waste form for disposal of secondary wastes from the Hanford waste treatment and immobilization plant. Cement and Concrete Research, 2013, 46, 14-22.	4.6	16
85	Chalcogen-Based Aerogels As Sorbents for Radionuclide Remediation. Environmental Science & Technology, 2013, 47, 7540-7547.	4.6	161
86	Iron phosphate glass for immobilization of 99Tc. Journal of Nuclear Materials, 2013, 441, 262-266.	1.3	21
87	Uptake Mechanism for Iodine Species to Black Carbon. Environmental Science & Technology, 2013, 47, 130827075129003.	4.6	20
88	Effects of Weathering Processes on Radioactive Cesium Sorption with Mineral Characterization in Korean Nuclear Facility Site. Journal of the Mineralogical Society of Korea, 2013, 26, 209-218.	0.2	4
89	Mineral dissolution and secondary precipitation on quartz sand in simulated Hanford tank solutions affecting subsurface porosity. Journal of Hydrology, 2012, 472-473, 159-168.	2.3	8
90	Characteristics of Cast Stone cementitious waste form for immobilization of secondary wastes from vitrification process. Journal of Nuclear Materials, 2012, 420, 164-174.	1.3	21

#	Article	IF	CITATIONS
91	Iron oxide waste form for stabilizing 99Tc. Journal of Nuclear Materials, 2012, 429, 201-209.	1.3	46
92	Changes in the pore network structure of Hanford sediment after reaction with caustic tank wastes. Journal of Contaminant Hydrology, 2012, 131, 89-99.	1.6	36
93	Strontium and Cesium Release Mechanisms during Unsaturated Flow through Waste-Weathered Hanford Sediments. Environmental Science & Technology, 2011, 45, 8313-8320.	4.6	21
94	Immobilization of 99-Technetium (VII) by Fe(II)-Goethite and Limited Reoxidation. Environmental Science & Technology, 2011, 45, 4904-4913.	4.6	124
95	Magnetic mesoporous materials for removal of environmental wastes. Journal of Hazardous Materials, 2011, 192, 1140-1147.	6.5	78
96	Characterization of uranium-contaminated sediments from beneath a nuclear waste storage tank from Hanford, Washington: Implications for contaminant transport and fate. Geochimica Et Cosmochimica Acta, 2010, 74, 1363-1380.	1.6	36
97	Resupply mechanism to a contaminated aquifer: A laboratory study of U(VI) desorption from capillary fringe sediments. Geochimica Et Cosmochimica Acta, 2010, 74, 5155-5170.	1.6	24
98	Transport of Strontium and Cesium in Simulated Hanford Tank Waste Leachate through Quartz Sand under Saturated and Unsaturated Flow. Environmental Science & Technology, 2010, 44, 8089-8094.	4.6	28
99	The effect of gravel size fraction on the distribution coefficients of selected radionuclides. Journal of Contaminant Hydrology, 2009, 107, 82-90.	1.6	4
100	Tomographic analysis of reactive flow induced pore structure changes in column experiments. Advances in Water Resources, 2009, 32, 1396-1403.	1.7	26
101	Uranium Phases in Contaminated Sediments below Hanford's U Tank Farm. Environmental Science & Technology, 2009, 43, 4280-4286.	4.6	42
102	Uranium(VI) sorption on iron oxides in Hanford Site sediment: Application of a surface complexation model. Applied Geochemistry, 2008, 23, 2649-2657.	1.4	38
103	Synthesis of nanoporous zirconium oxophosphate and application for removal of U(VI). Water Research, 2007, 41, 3217-3226.	5.3	45
104	Surface Complexation Modeling of U(VI) Sorption to Hanford Sediment with Varying Geochemical Conditions. Environmental Science & amp; Technology, 2007, 41, 3587-3592.	4.6	33
105	Sulfurâ€Functionalized Mesoporous Carbon. Advanced Functional Materials, 2007, 17, 2897-2901.	7.8	251
106	U(VI) adsorption on aquifer sediments at the Hanford Site. Journal of Contaminant Hydrology, 2007, 93, 255-269.	1.6	32
107	Enhanced Radionuclide Immobilization and Flow Path Modifications by Dissolution and Secondary Precipitates. Journal of Environmental Quality, 2005, 34, 1404-1414.	1.0	21
108	Sorption and transport behavior of radionuclides in the proposed low-level radioactive waste disposal facility at the Hanford site, Washington. Radiochimica Acta, 2005, 93, 57-63.	0.5	40

#	Article	IF	CITATIONS
109	Dendritic Chelating Agents. 1. Cu(II) Binding to Ethylene Diamine Core Poly(amidoamine) Dendrimers in Aqueous Solutions. Langmuir, 2004, 20, 2640-2651.	1.6	200
110	Metal Ion Sorption and Desorption on Zeolitized Tuffs from the Nevada Test Site. Environmental Science & Technology, 2004, 38, 496-502.	4.6	18
111	Linearity and reversibility of iodide adsorption on sediments from Hanford, Washington under water saturated conditions. Water Research, 2004, 38, 2009-2016.	5.3	57
112	Measuring the specific surface area of natural and manmade glasses: effects of formation process, morphology, and particle size. Colloids and Surfaces A: Physicochemical and Engineering Aspects, 2003, 215, 221-239.	2.3	42
113	Sorption mechanisms of Sr and Pb on zeolitized tuffs from the Nevada test site as a function of pH and ionic strength. American Mineralogist, 2003, 88, 2028-2039.	0.9	21